2024 IEEE International Conference on Microwaves, Communications, Antennas, Biomedical Engineering and Electronic Systems (COMCAS)

2024 IEEE International Conference on Microwaves, Communications, Antennas, Biomedical Engineering and Electronic Systems (COMCAS) | 979-8-3503-4818-7/24/$31.00 ©2024 IEEE | DOI: 10.1109/COMCAS58210.2024.10666205

A Wideband Dual-Polarized Stacked Patch Antenna Using Metasurface for 5G mmWave Application

Lintao Li, Yejun He*, Long Zhang, and Wenting Li

State Key Laboratory of Radio Frequency Heterogeneous Integration
Sino-British Antennas and Propagation Joint Laboratory
Guangdong Engineering Research Center of Base Station Antennas and Propagation
Shenzhen Key Laboratory of Antennas and Propagation
College of Electronics and Information Engineering, Shenzhen University, 518060, China
Email: 2110436067@szu.edu.cn, heyejun@126.com*, longzhang717@163.com, 525645594@qq.com

***Abstract*—A dual-polarization broadband metasurface antenna is presented in this paper. After stacked patches with 3×3 metasurfaces and an orthogonal aperture-coupling structure as well as air cavity structure are loaded, two patch modes and a slot mode are introduced and a broadband effect is obtained. Simulation results indicate that the proposed dual-polarization antenna achieves a relative bandwidth of over 55% in both polarization directions and maintains a small size and low profile. The average gain is 6.6 dBi across the entire operating frequency range.**

***Index Terms*—5G millimeter wave, metasurface, dual polarization, wideband.**

I. Introduction

In the modern communication system, the pursuit of high-speed transmission and large data capacity has spurred the rapid development of 5G millimeter-wave communication technology. Sub-6GHz 5G technology provided both higher speed data transmission and greater communication capacity. Millimeter-wave communication, as a pivotal component of 5G communication, offers heightened spectrum utilization and transmission rates. However, it also confronts limitations such as short propagation distances and weaker penetration capabilities. To surmount these challenges, researchers are dedicated to advancing antenna technology to support stable and reliable millimeter-wave communication.

In recent years, the 5G millimeter-wave frequency bands, including 24.25-27.5 GHz and 37.5-43 GHz, have been preliminarily earmarked as the primary frequency bands for Chinese 5G communication. Against this backdrop, dual-frequency antennas and broadband antennas, due to their small footprint, cost-effectiveness, and high integration, have emerged as notably scrutinized options.

A variety of dual-band and wideband antennas such as magnetoelectric dipole antenna [1], dielectric resonator antenna [2], multi-size patch antenna [3] and slot antenna [4] and so on have been proposed for millimeter wave communication. Recently, the metasurface antenna has attracted significant attention from researchers due to its unique advantages in expanding bandwidth and improving gain. As a radiator, a metasurface exhibits both a stable surface wave and a flexible ability to manipulate electromagnetic waves. In recent years, many works of metasurface millimeter wave antennas have been reported [5-7]. Utilizing metasurface structures to generate multiple modes for designing broadband or multi-frequency antennas is a commonly employed method. In [8], the diagonal, edge, and center patches of the 3×3 metasurface are modified to generate three resonant modes, achieving the objective of designing a dual-wideband antenna. In [9-10], the authors employ a combination of metasurface mode and slot mode to design a wideband antenna. However, for metasurface antennas, it is still a challenge for antenna designers to design a dual-polarization wideband millimeter wave antenna due to the limitations of the feeding structure of metasurface antennas.

In this paper, a dual-polarized wideband metasurface antenna fed by slot-coupling feeding technique is presented. The double-layer patch structure composed of a metasurface and a driven patch brings three resonance modes for the proposed antenna with broadband effect. Section II introduces the antenna design. Simulation results and discussion of the proposed antenna are presented in Section III. Section IV is the conclusion.

II. Antenna Design

A. Antenna structure

The three-dimensional model and layer configuration of the proposed antenna are shown in Fig. 1. The antenna consists of three layers of substrates: the first layer (Substrate 1) uses Rogers RT5880 with a relative dielectric constant of 2.2 and a loss tangent of 0.0009, and the second layer (Substrate 2) and the third layer (Substrate 3) apply FR4 with a relative dielectric constant of 4.4 and a loss tangent of 0.02. FR4 is an economical and practical material with a high dielectric constant. Substrate 3 is made by pressing two layers of FR4 plates of different thicknesses. This proposed antenna adopts the multilayer PCB manufacturing process, and the aperture-coupling feeding structure adopts an FR4 plate to reduce the cost and antenna size.

The metasurface and driven patch are printed on the upper and lower layers of Substrate 1, respectively. Compared to single-layer metasurface, stacked patches loaded with metasurface have a smaller size and greater design freedom. The

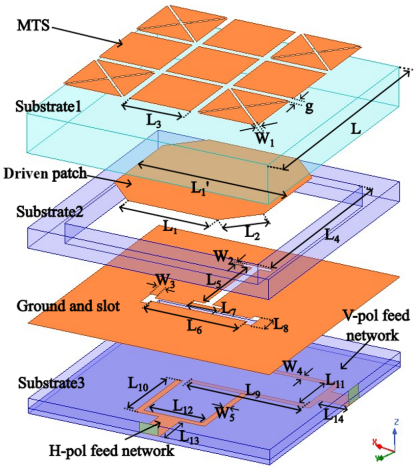

(a) 3D view of proposed antenna.

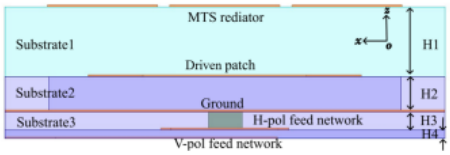

(b) Side view of proposed antenna.

Fig. 1: Structures of proposed antenna.

metasurface is composed of a 3×3 patch array, where each diagonal patch is divided into four smaller triangles to enhance impedance matching and improve antenna gain. The four corners of the driven patch are chamfered to get better impedance match. The center position of Substrate 2 is cut into an air cavity to reduce the high loss tangent of the FR4 board and widen the antenna bandwidth. The feeding structure of the antenna adopts asymmetric feeding scheme, where two orthogonal H-shaped slots are etched on the ground and two Y-shaped feeders are printed on different planes. The size of a single antenna is $0.55\lambda_0 \times 0.55\lambda_0 \times 0.16\lambda_0$, which has the advantage of low profile. The optimized parameters of the proposed antenna are shown in Table I.

TABLE I: Geometric Parameters (unit:*mm*)

Parameters	L	L_1	L_1'	L_2	L_3	L_4
value	5	1.86	3.1	0.88	1.25	4
Parameters	L_5	L_6	L_7	L_8	L_9	L_{10}
value	1.8	2	0.6	0.4	2.4	1.5
Parameters	L_{11}	L_{12}	L_{13}	L_{14}	W_1	W_2
value	0.98	1.22	0.68	0.58	0.05	0.1
Parameters	W_3	W_4	W_5	H_1	H_2	H_3
value	0.15	0.12	0.12	0.787	0.4	0.2
Parameters	H_4	g				
value	0.1	0.14				

B. Design Steps of the proposed antenna

In order to explain the working principle of the proposed antenna, three reference antennas are introduced. All three

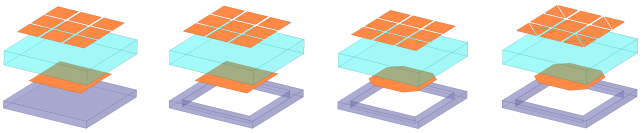

(a) Ant 1. (b) Ant 2. (c) Ant 3. (d) Proposed.

Fig. 2: Evolutionary design steps of the proposed antenna.

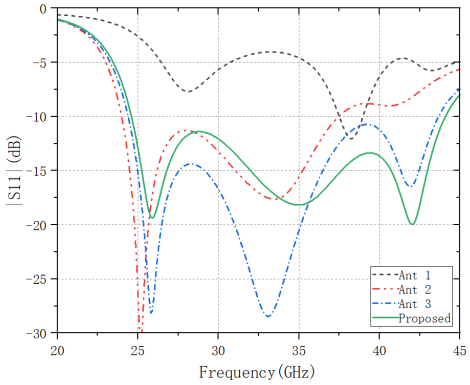

(a) $|S_{11}|$ of reference antennas and proposed antenna.

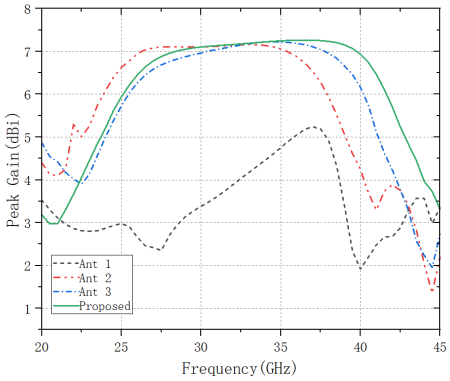

(b) Peak gain of reference antennas and proposed antenna.

Fig. 3: Simulation results of reference antennas and proposed antenna.

reference antennas and proposed antenna as shown in Fig. 2 (a)-(d) utilize the same aperture-coupled feeding structure. Thus, for the convenience of viewing, only the modified antenna structures are shown.

Figure 3 illustrates the $|S_{11}|$ parameters and gain curves of the proposed antenna and the reference antennas. Reference Ant 1, depicted in Fig. 2 (a), features a simple dual-layer patch structure loaded with a 3×3 metasurface. As seen in Fig. 3 (b), due to the high-loss characteristics of FR4, Ant 1 exhibits lower gain and poor matching bandwidth. On the basis of Ant 1, an air cavity is introduced at the center of Substrate 2 to design reference Ant 2. The introduced air cavity effectively reduces the loss tangent of FR4, resulting in a substantial gain enhancement and improved impedance matching. Reference Ant 3 employs chamfered corners on the driven patch, shifting the third resonance point to a higher frequency, thus broad-

ening the impedance bandwidth. In comparison to reference Ant 3, the proposed antenna further cuts each diagonal patch of the metasurface into four smaller triangles, shifting the second resonance point to a higher frequency, and overall elevating the antenna gain.

C. Parameter studies of the proposed antenna

As shown in Fig. 4, the proposed antenna has three resonant points at 26 GHz, 35 GHz, and 42 GHz, which represent three resonant modes of the antenna, respectively. Next, parameter sweeps were conducted for the length of metasurface, driven patch and feeding slot to analyze the influence of these three parameters on the antenna resonant points. Figure 4 shows how the $|S_{11}|$-parameters of the antenna are changed when some sizes are modified. When the size of the 3×3 metasurface is altered, the position of the second resonant point is changed, while the position of the other two resonant points remains unchanged, which indicates that the metasurface mainly determines the position of the second resonant point of the antenna. When modifying the size of the driven patch, only the position of the third resonant point of the antenna has been changed significantly. Therefore, the third resonant point of the antenna is mainly determined by the driven patch. The position of the first resonant point is mainly determined by the length of the slot of the aperture-coupled feeding structure, which indicates that this is a slot mode brought by the feeding structure. By modifying these three sizes of the proposed antenna, the three resonance points of the proposed antenna can be independently adjusted.

In combination with the above discussion, it can be concluded that the stacked patch structure of the proposed metasurface antenna brings two modes at 35 GHz and 42 GHz, while the feeding structure brings a slot mode at 26 GHz. Figure 5 shows the current distribution of the proposed antenna at 26 GHz, 35 GHz, and 42 GHz. As shown in Fig. 5, the current of the slot mode is mainly distributed at the edge of the driven patch and metasurface. At 35 GHz, the metasurface antenna and the drive patch current are in the same direction. However, at 42 GHz, the metasurface antenna and the driven patch current are in the opposite direction.

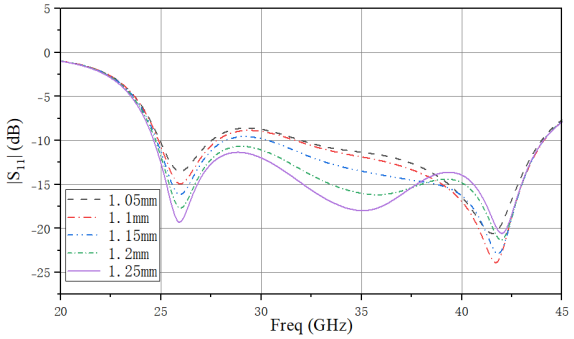

(a) Effect of modifing the length(L_3) of metasurface.

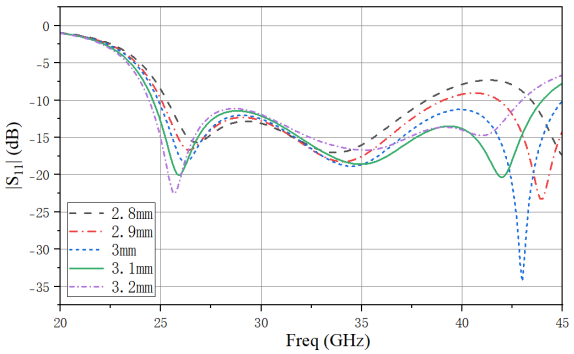

(b) Effect of modifing the length(L_1') of driven patch.

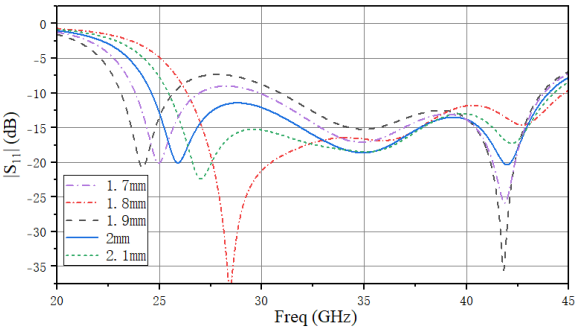

(c) Effect of modifing the length(L_6) of slot.

Fig. 4: S-parameter of different parameters.

III. Simulation Results And Discussion

Figure 6 shows the S-parameter and gain of the proposed antenna. The -10 dB impedance bandwidths of the two polarizations are 24.69-44.26 GHz and 24.65-43.42 GHz, respectively. This signifies that the antenna boasts a relative bandwidth exceeding 55% for both polarizations, effectively covering the entire range of 5G millimeter-wave communication frequencies from 25 GHz to 43 GHz. The aperture-coupling feeding slots placed orthogonally result in a great port isolation degree in the whole working band. The antenna port isolation degree is greater than 25 dB.

In the frequency range of 25 GHz to 43 GHz, the proposed antenna has a flat gain curve in the passband, achieving the gains of 4.66 to 7.2 dBi, with an average gain of 6.6 dBi. Figure 7 shows the pattern of the proposed antenna at 26 GHz,

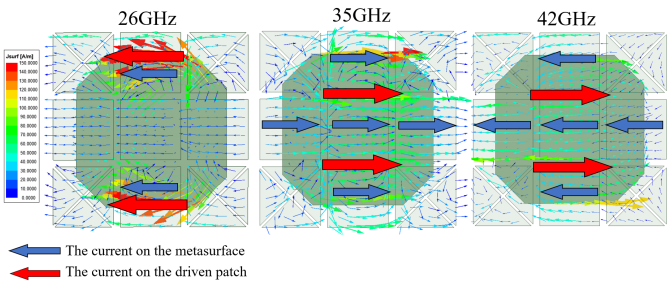

Fig. 5: Current distribution at 26 GHz (slot mode),35 GHz and 42 GHz (patch modes).

33 GHz, and 40 GHz. The cross-polarization isolation degree of the main polarization direction antenna is greater than

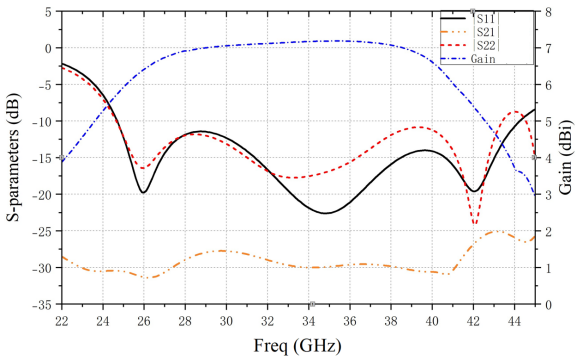

Fig. 6: S parameters and gain of proposed antenna.

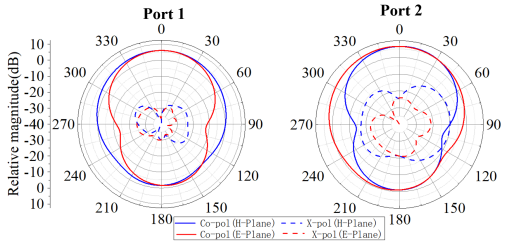

(a) Radiation patterns at 26 GHz.

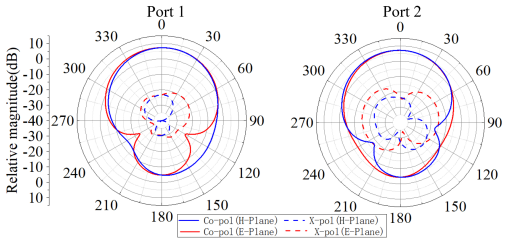

(b) Radiation patterns at 33 GHz.

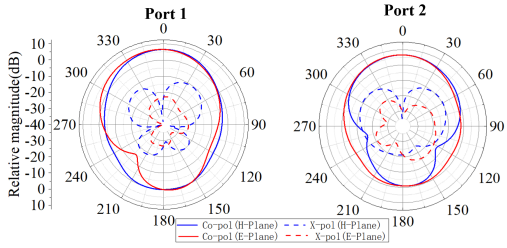

(c) Radiation patterns at 40 GHz.

Fig. 7: Radiation patterns of proposed antenna.

20 dBi, indicating that the radiation pattern of the proposed antenna has good directivity and stability. In addition, due to the asymmetric feeding structure, the pattern of the proposed antenna has some skews in the working frequency band. Thus, it is necessary to design a suitable feeding network to reduce the impact of antenna elements during array formation.

IV. Conclusion

A dual-polarized wideband metasurface antenna is proposed. By using metasurface and the design method of aperture-coupling feeding structure and cavity, the relative bandwidth of the two polarizations of the proposed antenna exceeds 55%, which can cover most of the frequency bands of 24.25 - 27.5 GHz and 37.5 - 43 GHz. The antenna has an average gain of 6.6 dBi and a stable radiation pattern in the operating frequency band. The antenna size is $0.55\lambda_0 \times 0.55\lambda_0 \times 0.16\lambda_0$, and has the advantages of low profile and small size. In addition, the base material part of the antenna selected an affordable FR4 plate, effectively reducing the overall cost of the antenna. In conclusion, the proposed antenna is an ideal candidate for 5G millimeter wave broadband base station antenna.

TABLE II: Comparison between the proposed design and other exsiting works.)

Ref.	BW (LB/HB) (%)	Gain (dBi)	Ant. size	Pol.
[1]	19.9/20.2	6.1/8.7	$0.69 \times 0.69 \times 0.17$	Single linear
[2]	42	6.1	$0.43 \times 0.43 \times 0.33$	Dual linear
[3]	29.15	6.3/8.9	$0.7 \times 0.7 \times 0.15$	Dual linear
[8]	20.7/11.3	7.2/10.9	$0.9 \times 0.9 \times 0.202$	Dual linear
[11]	23.9	4.5	$0.35 \times 0.49 \times 0.21$	Dual linear
[12]	43.1	6.12	$0.348 \times 0.348 \times 0.07$	Dual linear
Proposed	55	7.2	$0.55 \times 0.55 \times 0.16$	Dual linear

Ref.: Reference; BW: Bandwidth; Ant.: Antenna; Pol.: Polarization.

Acknowledgment

This work is supported in part by the National Natural Science Foundation of China (NSFC) under Grants 62071306 and 61801299, and in part by Shenzhen Science and Technology Program under Grants JSGG20210802154203011, JCYJ20200109113601723 and JSGG20210420091805014.

References

[1] S. Ni, X. Li, X. Qiao, Q. Wang and J. Zhang, "A Compact Dual-Wideband Magnetoelectric Dipole Antenna for 5G Millimeter-Wave Applications," *IEEE Transactions on Antennas and Propagation*, vol. 70, no. 10, pp. 9112-9119, Oct. 2022.

[2] J. Kowalewski, J. Eisenbeis, A. Jauch, J. Mayer, M. Kretschmann and T. Zwick, "A mmW Broadband Dual-Polarized Dielectric Resonator Antenna Based on Hybrid Modes," *IEEE Antennas and Wireless Propagation Letters*, vol. 19, no. 7, pp. 1068-1072, Jul. 2020.

[3] X. Tong, Z. H. Jiang, C. Yu, F. Wu, X. Xu and W. Hong, "Low-Profile, Broadband, Dual-Linearly Polarized, and Wide-Angle Millimeter-Wave Antenna Arrays for Ka-Band 5G Applications," *IEEE Antennas and Wireless Propagation Letters*, vol. 20, no. 10, pp. 2038-2042, Oct. 2021.

[4] W. Liu and S. Yan, "A Design of Millimeter-Wave Dual-Polarized SIW Phased Array Antenna Using Characteristic Mode Analysis," *IEEE Antennas and Wireless Propagation Letters*, vol. 21, no. 1, pp. 29-33, Jan. 2022.

[5] F. H. Lin and Z. N. Chen, "Low-Profile Wideband Metasurface Antennas Using Characteristic Mode Analysis," *IEEE Transactions on Antennas and Propagation*, vol. 65, no. 4, pp. 1706-1713, Apr. 2017.

[6] T. Li and Z. N. Chen, "Design of Dual-Band Metasurface Antenna Array Using Characteristic Mode Analysis (CMA) for 5G Millimeter-Wave Applications," in *Pro. 2018 IEEE-APS Topical Conference on Antennas and Propagation in Wireless Communications (APWC)*, Cartagena, Colombia, 2018, pp. 721-724.

[7] S. Liu, D. Yang, Y. Chen, K. Sun, X. Zhang and Y. Xiang, "Low-Profile Broadband Metasurface Antenna Under Multimode Resonance," *IEEE Antennas and Wireless Propagation Letters*, vol. 20, no. 9, pp. 1696-1700, Sept. 2021.

[8] T. Li and Z. N. Chen, "A Dual-Band Metasurface Antenna Using Characteristic Mode Analysis," *IEEE Transactions on Antennas and Propagation*, vol. 66, no. 10, pp. 5620-5624, Oct. 2018.

[9] F. H. Lin and Z. N. Chen, "Low-profile wideband metasurface antennas using characteristic mode analysis," *IEEE Transactions on Antennas and Propagationg*, vol. 65, no. 4, pp. 1706-1713, Apr. 2017.

[10] J. -W. Lian, D. Ding and R. Chen, "Wideband Millimeter-Wave Substrate-Integrated Waveguide-Fed Metasurface Antenna," *IEEE Transactions on Antennas and Propagation*, vol. 70, no. 7, pp. 5335-5344, Jul. 2022.

[11] R. Lu et al., "SIW Cavity-Fed Filtennas for 5G Millimeter-Wave Applications," *IEEE Transactions on Antennas and Propagation*, vol. 69, no. 9, pp. 5269-5277, Sept. 2021.

[12] D. Chen, Q. Xue, W. Yang, K. -S. Chin, H. Jin and W. Che, "A Compact Wideband Low-Profile Metasurface Antenna Loaded With Patch-Via-Wall Structure," *IEEE Antennas and Wireless Propagation Letters*, vol. 22, no. 1, pp. 179-183, Jan. 2023.